



Contents lists available at ScienceDirect

Bioorganic & Medicinal Chemistry Letters

journal homepage: www.elsevier.com/locate/bmcl



Discovery of a potent and selective Bcl-2 inhibitor using SAR by NMR

Andrew M. Petros, Jeffrey R. Huth, Thorsten Oost, Cheol-Min Park, Hong Ding, Xilu Wang, Haichao Zhang, Paul Nimmer, Renaldo Mendoza, Chaohong Sun, Jamey Mack, Karl Walter, Sarah Dorwin, Emily Gramling, Uri Lador, Saul H. Rosenberg, Steven W. Elmore, Stephen W. Fesik, Philip J. Hajduk*

Global Pharmaceutical Research and Development, Abbott Laboratories, Abbott Park, IL 60064, United States

ARTICLE INFO

Article history:

Received 12 August 2010

Revised 1 September 2010

Accepted 7 September 2010

Available online 15 September 2010

Keywords:

NMR

Structure-based

Linking

Fragment

Apoptosis

Bcl

ABSTRACT

The Bcl-2 family of proteins plays a major role in the regulation of apoptosis, or programmed cell death. Overexpression of the anti-apoptotic members of this family (Bcl-2, Bcl-x_L, and Mcl-1) can render cancer cells resistant to chemotherapeutic agents and therefore these proteins are important targets for the development of new anti-cancer agents. Here we describe the discovery of a potent, highly selective, Bcl-2 inhibitor using SAR by NMR and structure-based drug design which could serve as a starting point for the development of a Bcl-2 selective anti-cancer agent. Such an agent would potentially overcome the Bcl-x_L mediated thrombocytopenia observed with ABT-263.

© 2010 Elsevier Ltd. All rights reserved.

Cancer is a complex disease that arises from a decades-long process of accumulated mutations. One hallmark of malignant cells is their ability to evade apoptosis, or programmed cell death.¹ There are many ways that cancer cells achieve this, one of which is through overexpression of one or more members of the Bcl-2 family of anti-apoptotic proteins. This family includes Bcl-2, Bcl-x_L, Bcl-w, Mcl-1, and A1. Recently, we have developed a potent, orally bioavailable, dual Bcl-x_L/Bcl-2 inhibitor (ABT-263) that shows robust in vivo activity against a number of different tumors.² While a very potent anti-tumor agent, this molecule suffers the drawback of inducing thrombocytopenia upon dosing.³ Furthermore, we have shown that this thrombocytopenia is mediated by inhibition of Bcl-x_L and not of Bcl-2.³ Resistance of cancer cells to apoptosis, on the other hand, is mediated by Bcl-x_L, Bcl-2, or both, depending on the tumor type. Therefore, a Bcl-2 selective inhibitor could have utility as a platelet-sparing anti-tumor agent.

Here, we report the use of SAR by NMR and structure-based drug design in the discovery of selective inhibitors of Bcl-2 based on a diphenylmethane core. These compounds have nanomolar potency against Bcl-2, but exhibit >1000-fold and >28-fold selectivity over Bcl-x_L and Mcl-1, respectively, and could serve as a useful starting point for development of a Bcl-2 selective, anti-tumor agent.

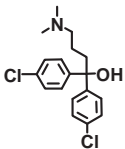
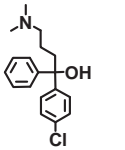
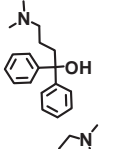
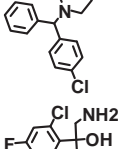
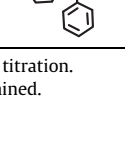
In order to identify ligands that could serve as starting cores in the development of Bcl-2 selective inhibitors, an NMR-based screen of human Bcl-2 was conducted using a library of about 17,000 compounds with an average molecular weight of 225 Da.⁴ Compound binding was monitored by following chemical shift changes of Leu, Val, and Ile methyl groups in a ¹³C-HSQC spectrum upon compound addition. A diphenylmethane (compound **1**, Table 1) was discovered that binds to Bcl-2 with a K_D of 20 μM, as measured in an NMR titration experiment. A similar compound has been discovered by Jahnke using an NMR spin-labeling method.⁵ Complementary titrations using Bcl-x_L found this compound to be 20-fold selective for Bcl-2 (Table 1) and it was, in fact, the only compound to show this degree of selectivity. This is in contrast to the binding profile of biaryl acid compounds that were previously discovered in a screen of Bcl-x_L.⁴ For example, biaryl acids (**6**, **7**, and **8**) bind with nearly equal affinity to both Bcl-2 family members (Table 2).

To understand the structural basis for this selectivity and to guide the design of more potent Bcl-2 selective inhibitors, NMR structural studies of compound **1** bound to Bcl-2 were conducted. NMR was chosen for these studies since we were not able, at the time, to obtain crystals of Bcl-2 in complex with compounds of micromolar affinity. Twelve protein–ligand NOEs were observed in a three-dimensional, ¹³C-edited, ¹²C-filtered NOESY spectrum (Supplementary data), which were then used to guide docking of **1** into the Bcl-2 groove. As shown in Figure 1, the chlorinated phenyl rings of **1** pack into the hydrophobic groove created by the side

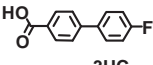
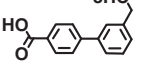
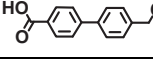
* Corresponding author. Address: Abbott Laboratories, Dept. R460, Bldg. AP10, 100 Abbott Park Rd., Abbott Park, IL 60064, United States. Tel.: +1 (847)937 0368; fax: +1 (847)938 2478.

E-mail address: philip.hajduk@abbott.com (P.J. Hajduk).

Table 1
NMR K_D values for diphenylmethanes

No.	Structure	K_D^a (μ M) Bcl-2	K_D^a (μ M) Bcl-x _L
1		20	450
2		80	500
3		200	5000
4		60	700
5		250	ND ^b

^a From NMR titration.^b Not determined.**Table 2**
NMR K_D values for biaryl acids

No.	Structure	Bcl-x _L K_D^a (μ M)	Bcl-2 K_D^a (μ M)	
			–1 ^b	+1 ^c
6		300	400	430
7		290	100	20
8		360	300	>1000

^a From NMR titration.^b No compound **1**.^c Compound **1** at 500 μ M.

chains of L116, V130, M112, and L134. The methane core positions the hydrophilic substituents away from the hydrophobic pocket towards the polar side chains of E111, D108, and E133 on the surface of the protein. Although we show the hydroxyl of **1** pointing towards E111, a binding orientation with this group interacting with E133, obtained by rotating compound **1** by approximately 180° in the pocket, is also consistent with the NMR NOE data. The diphenylmethane SAR is consistent with this NMR-derived structure (Table 1). Removal of one (**2**) or both (**3**) chlorines weakens binding by 4- and 10-fold, respectively, as would be expected from reduced hydrophobic interactions with the groove. On the other hand, the hydroxyl and dimethylpropylamine seem to be less critical for binding. For example, replacing them with a methylpiperazine leads to a compound with equal affinity (compare **4** with **2**). From the structure, it is clear that a variety of polar substitutions from the diphenylmethane core would be able to interact with the flexible polar side chains on the protein surface.

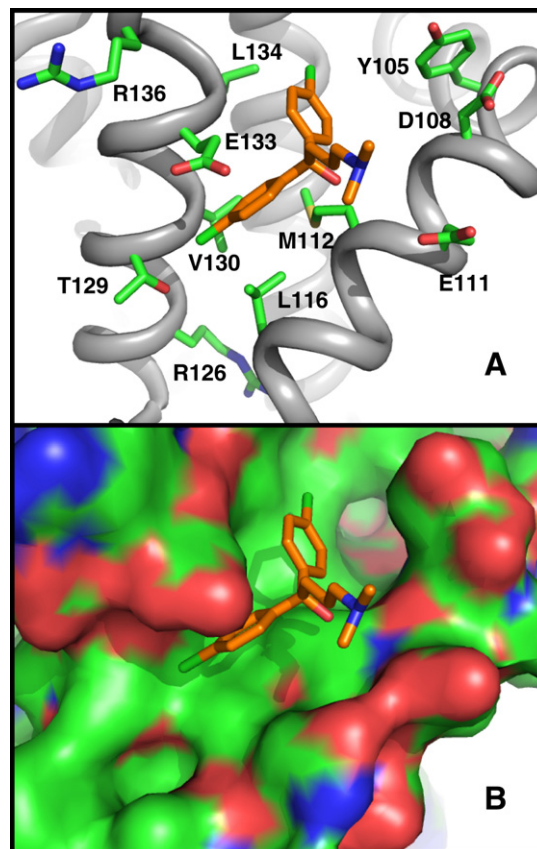


Figure 1. NMR-derived structure of diphenylmethane compound **1** bound to Bcl-2. (A) Ribbon representation. Amino acid side chains that form the binding pocket are indicated with carbon in green, nitrogen in blue, sulfur in orange, and oxygen in red. Atoms of the ligand are colored with carbon in orange, oxygen in red, nitrogen in blue, and chlorine in green. (B) Bcl-2 surface is shown in green with oxygen atoms in red and nitrogen atoms in blue.

Based on the NMR-derived structure, a strategy was pursued to extend the diphenylmethane core into the unoccupied region of the groove in order to improve potency. A structural comparison of the Bcl-2/diphenylmethane complex with the Bcl-x_L/biaryl acid complex⁴ suggested that the diphenylmethane and biaryl acid ligands would occupy neighboring sites in the Bcl-2 groove and could thus bind simultaneously. To test this hypothesis, 70 biaryl acids were screened for binding to a complex of Bcl-2 and compound **1**. As the data in Table 2 show, the *para*-fluoro substituted biaryl (**6**) binds equally as well to Bcl-2 in the presence and absence of the diphenylmethane. No evidence for competition for binding to the same site was observed. The larger ethyl group at the *meta* position binds fourfold more tightly (compound **7**). Furthermore, the ethyl substitution may favorably interact with the diphenylmethane as evidenced by the fivefold increase in potency when compound **1** is present versus when it is absent. In contrast, an ethyl substitution at the *para* position (**8**) seems to inhibit binding in the presence of **1** but not in its absence. This suggests steric clash between the two ligands when bound to Bcl-2. Overall, the SAR for binding of biaryl acids in the presence of **1** is consistent with the hypothesis that both ligands bind proximal to one another in the Bcl-2 ligand-binding groove.

NMR structural studies of a ternary complex between a biaryl acid and a diphenylmethane were undertaken to confirm the binding orientation. To identify a ternary complex for which strong intermolecular NOEs could be measured, 14 ternary complexes were evaluated using 2D ¹³C-filtered NOESY experiments. First, eight different biaryl acids were prepared in complex with Bcl-2

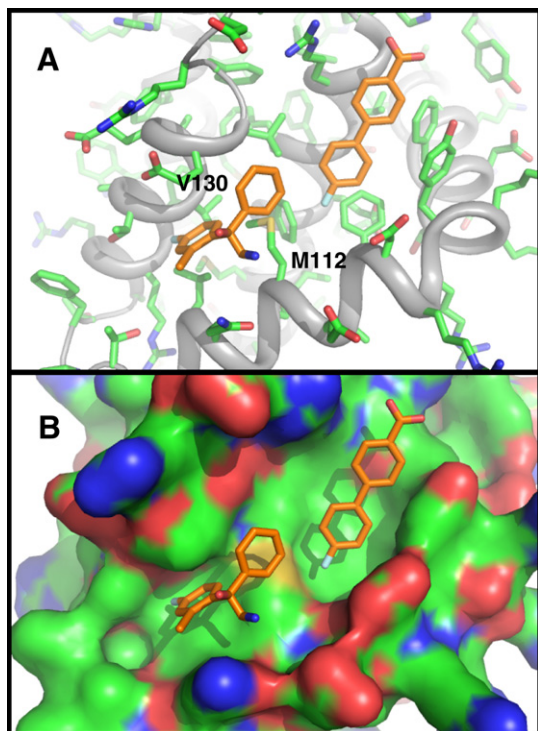


Figure 2. NMR-derived structure of a ternary complex of Bcl-2 with compounds **5** and **6**. (A) Ribbon representation with color coding as described in Figure 1. (B) Bcl-2 surface with coloring as described in Figure 1. Ligand atoms are colored with carbon in orange, oxygen in red, nitrogen in blue, chlorine in green, and fluorine in cyan.

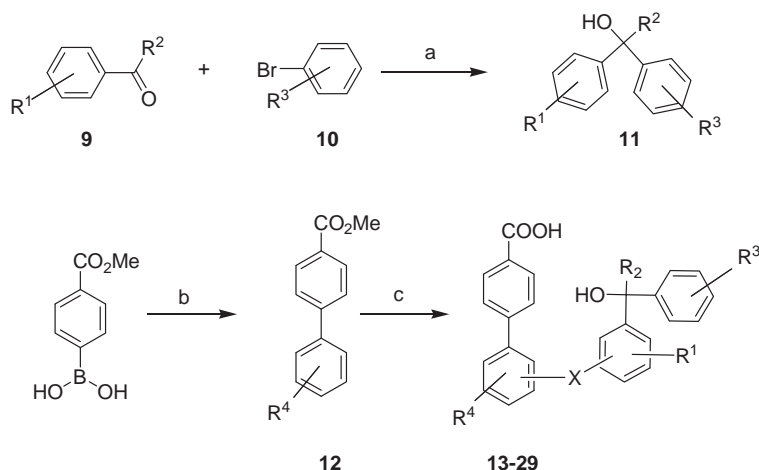
and compound **1**. Of these, the *para*-fluoro and *para*-methyl substituted biaryl acids yielded the highest quality 2D filtered NOE spectra, based on NOE intensity and chemical dispersion of compound aromatic protons. Next, these acids were evaluated in ternary complexes with three other analogs of **1**. A ternary complex between **5** and **6** yielded the highest quality spectra. From a three-dimensional, ^{13}C -edited, ^{12}C -filtered NOESY spectrum, a total of 32 intermolecular NOEs between the ligands and Bcl-2 were observed. The ligands were docked into the Bcl-2 groove using these intermolecular NOEs and minimized using Xplor.⁶ As shown in Figure 2, the diphenylmethane in the ternary complex binds to the same pocket

as it does in the absence of the biaryl acid (Fig. 1). Furthermore, the biaryl binds further up the groove with its fluorophenyl pointing towards the diphenylmethane. This orientation is consistent with the biaryl SAR where *meta* and *para* substitutions seem to interact favorably or clash with the diphenylmethane, respectively. Both the structural studies (Fig. 2) and biaryl SAR (Table 2) indicated that linking the two ligands could be achieved from the *para* or *meta* position of the biaryl. Similarly, both the *meta*- and *para*-positions of the diphenylmethane could direct a linker towards the biaryl.

To investigate this linking strategy, two-, three-, and four-atom linkers were evaluated at the *meta*- and *para*-positions of each fragment using the general synthetic strategy outlined in Scheme 1. Variations in the diphenyl methane core were explored through routine reaction of appropriate beta-amino ketones (**9**) with various aryl bromides (**10**) (Scheme 1) to yield intermediate diphenylmethane derivatives (**11**) with either a *meta*- or *para*-hydroxyl group. The biaryl ester portion of the molecules (**12**) was then assembled through simple Suzuki couplings of 4-(methoxycarbonyl)phenylboronic acid with different aryl bromides. A subsequent Mitsunobu coupling of the core moieties yielded target compounds **13–29**.

These compounds were then evaluated in a fluorescence polarization competition assay, using a fluorescently-labeled peptide from the anti-apoptotic protein Bad as a probe.⁷ These data are summarized in Tables 3 and 4. Several linking strategies produced compounds with inhibition constants in the low micromolar range indicating a favorable linking geometry. Because *meta/para* and *para/meta* two- and three-atom linkers yielded compounds with similar potencies, we can conclude that some flexibility in binding exists. This variability is likely enhanced by the absence of the phenyl-substitutions that contribute to binding of the diphenylmethane core (Tables 1 and 2).

When hydrophobic substitutions were added back to the diphenylmethane core in the linked compounds, potency improved as expected. Dichloro-substitutions improved the potency of the linked compound by 10-fold (**24** and **25**, Table 4). The majority of this improvement came from the chloro groups and not modification of the dimethylamine in **24**. This conclusion is consistent with the observation that compounds with and without the polar morpholino group differed by at most twofold in potency (**25** and **26**). The same SAR was observed for the unlinked diphenylmethanes. Addition of two chlorines improved potency by 10-fold (**1** and **3**, Table 1), while the substitution of the dimethyl amine with a



Scheme 1. General synthesis of linked biaryl acid inhibitors. Reagents and conditions: (a) substituted 2-amino ketone (**9**), substituted bromobenzene (**10**), $n\text{BuLi}$, THF, -78°C . (b) Suzuki coupling: substituted bromobenzene, $\text{Pd}(\text{dppf})$, aq Cs_2CO_3 , dioxane, 4-(methoxycarbonyl)phenylboronic acid. (c) Mitsunobu: DIAD, PPH_3 , THF, **11**.

Table 3
Influence of linker length and geometry on Bcl-2 inhibition

No.	Structure	K_i^a (μ M)
13		5.0
14		20
15		5.2
16		4.6
17		3.4
18		>1
19		5.8
20		8.0
21		83
22		12
23		>1

^a Fluorescence polarization assay.**Table 4**
Activity of linked compounds

No.	Structure	K_i^a (μ M)
24		34
25		0.22
26		0.46
27		0.20
28		0.11
29		0.04

^a Fluorescence polarization assay.

piperazine (**2** and **4**) had little effect on affinity. In order to further improve potency using structure-based design, binding of **27** was studied by NMR. A total of 46 protein–ligand NOEs were used to dock **27** into the groove of Bcl-2 (Fig. 3). The biaryl and diphenylmethane components were found to bind to the same pockets as in the ternary complex. Unexpectedly, however, the binding positions in these pockets changed dramatically. In the presence of the linked compound, the side chain of M112 moves away from V130 creating a deeper pocket (compare Figs. 2A and 3A). This is accompanied by reorientation of the diphenylmethane (Fig. 3B) such that one chlorophenyl fills the pocket vacated by the M112

methyl group. The biaryl also moves closer to V130 in the linked compound. These structural results explain the linker SAR that was observed (Table 3). The ability of long, narrow hydrophobic compounds to slide within the Bcl-2 hydrophobic groove is consistent with multiple linker lengths and linker geometries being compatible with this pocket. In addition to explaining the SAR of compound linking, further improvement in potency could be obtained by increasing the size of the *para*-substituent on the distal ring of the diphenylmethane (Fig. 3). Consistent with this prediction, a bulky *t*-butyl improved potency further to 0.11 μ M (**28**).

The structure of **27** also indicated that additional interactions with the Bcl-2 groove could be accessed from the biaryl. A limited number of compounds were made to explore this possibility, but none showed improved affinity over the unsubstituted analogs. In addition, acid replacements that preserved a negative charge, such as a tetrazole or acylsulfonamide, were equipotent. However, uncharged compounds where the carboxyl was replaced with an alcohol, nitrile, or methyl ester were inactive. In fact, this SAR is consistent with the SAR of biaryl-containing inhibitors of Bcl-x_L in that an unsubstituted biaryl acid seems to optimally fill this region of the BH3-binding groove.⁴ Finally, the binding affinity of the linked compound was improved to 0.04 μ M by replacing the

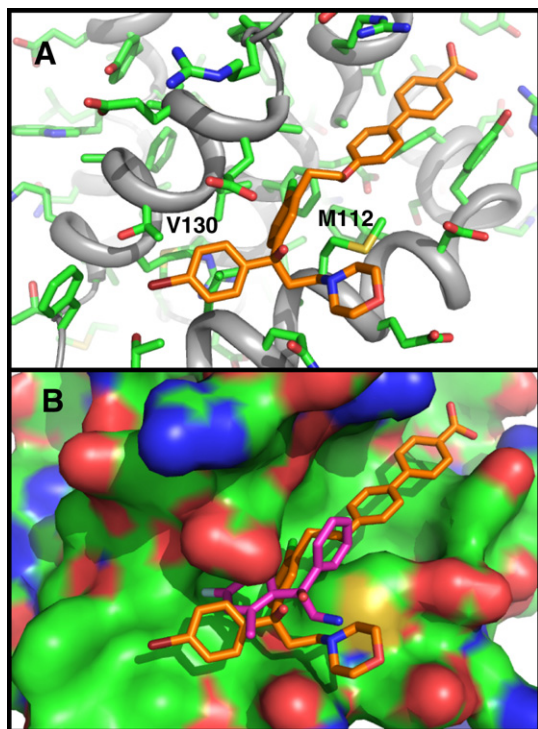


Figure 3. NMR-derived structure of Bcl-2 in complex with compound **27**. (A) Ribbon representation with color coding for Bcl-2 as described in Figure 1. Atoms of the ligand are colored with carbon in orange, oxygen in red, nitrogen in blue, chlorine in magenta, and bromine in brown. (B) Surface representation including **1** superimposed on **27**. Bcl-2 is colored as described in Figure 2B. For **27**, carbon atoms are in orange, oxygens in red, nitrogen in blue, chlorine in magenta, and bromine in brown. For **1**, carbon and atoms are in magenta, oxygen in red, and nitrogen in blue.

morpholino group of **28** with a pyrrolidine (**29**). A structural explanation for this gain in potency is not apparent from the structure of **27** (Fig. 3). Polar interactions with surface amino acids E111, Q115, or E133, may be important. However, NMR structural studies of a pure enantiomer would need to be pursued to understand the details of the pyrrolidine interaction.

The theoretical gain in potency for the linking of two compounds is simply the product of the dissociation constants for the individual compounds plus a contribution from the linker itself, the latter of which is difficult to quantify. Thus optimal linking of **1** ($K_D = 20 \mu\text{M}$) with **6** ($K_D = 400 \mu\text{M}$) would give a K_D of at least 8 nM. The linked compound **25** most closely represents the original ligands and with an inhibition constant of 220 nM is about 27-fold weaker than the theoretical value. This difference most likely arises from the inability to maintain the optimal position of the individual compounds given the constraint of finite bond lengths and finite angles in the linker.

NMR-based fragment binding studies of the dichlorodiphenyl methane indicated that this core is 20-fold specific for Bcl-2 over Bcl-x_L (Table 1). To determine whether this specificity was preserved when linked to the biaryl acid, compound **29** was tested against a panel of anti-apoptotic Bcl-2 family proteins, including Bcl-x_L, in a fluorescence polarization assay.⁷ Consistent with the results for binding of the diphenylmethane fragment, **29** is more than 1000-fold more potent against Bcl-2 versus Bcl-x_L. A structural

rationale for this difference may be the presence in Bcl-x_L of a leucine residue at position 112 as opposed to the methionine residue in Bcl-2. The sidechain of this methionine flips out of the groove in order to accommodate the chlorophenyl ring of **29**. Such sidechain movement is not possible for the more rigid leucine of Bcl-x_L. Similarly, greater than 1000-fold specificity was observed for Bcl-2 versus Bcl-w, greater than 100-fold versus Bcl-B, about 58-fold versus A1, and about 28-fold versus Mcl-1. This is in contrast to the specificity profile of ABT-737 that binds with sub-nanomolar affinity to Bcl-2, Bcl-x_L, and Bcl-w, but with micromolar affinity to Mcl-1, Bcl-B, and A1.⁸ To date, this is the first potent small molecule inhibitor to be described which is highly selective for Bcl-2.⁹

The potency of **29** in killing Bcl-2 dependent tumor cells was evaluated using a Bcl-2 dependent follicular lymphoma cell line (FL12).⁸ An EC_{50} of 16 μM was determined for this cell line, which based on our experience with ABT-737 and ABT-263 analogs, is consistent with a K_i of 0.04 μM . Given this cellular potency it is unlikely that these compounds would be active in vivo. However, they may serve as a useful starting point for developing a potent, Bcl-2 selective, anti-tumor agent. Further gains in potency could potentially be achieved by replacing the carboxylate moiety with an acylsulfonamide and then building off of this acylsulfonamide to fill unoccupied portions of the groove in a manner similar to ABT-737.⁴

Acknowledgment

Thanks to Steve Swann for assistance in preparing this manuscript.

Supplementary data

Supplementary data associated with this article (protein expression and procedures for NMR structural studies) can be found, in the online version, at doi:10.1016/j.bmcl.2010.09.033.

References and notes

- Hanahan, D.; Weinberg, R. A. *Cell* **2000**, 100, 57.
- Tse, C.; Shoemaker, A. R.; Adickes, J.; Anderson, M. G.; Chen, J.; Jin, S.; Johnson, E. F.; Marsh, K. C.; Mitten, M. J.; Nimmer, P.; Roberts, L.; Tahir, S. K.; Xiao, Y.; Yang, X.; Zhang, H.; Fesik, S.; Rosenberg, S. H.; Elmore, S. W. *Cancer Res.* **2008**, 68, 3421.
- Zhang, H.; Nimmer, P. M.; Tahir, S. K.; Chen, J.; Fryer, R. M.; Hahn, K. R.; Iciek, L. A.; Morgan, S. J.; Nasarre, M. C.; Nelson, R.; Preusser, L. C.; Reinhart, G. A.; Smith, M. L.; Rosenberg, S. H.; Elmore, S. W.; Tse, C. *Cell Death Differ.* **2007**, 14, 943.
- Petros, A. M.; Dinges, J.; Augeri, D. J.; Baumeister, S. A.; Betebenner, D. A.; Bures, M. G.; Elmore, S. W.; Hajduk, P. J.; Joseph, M. K.; Landis, S. K.; Nettesheim, D. G.; Rosenberg, S. H.; Shen, W.; Thomas, S.; Wang, X.; Zanze, I.; Zhang, H.; Fesik, S. W. *J. Med. Chem.* **2006**, 49, 656.
- Jahnke, W. *ChemBioChem* **2002**, 3, 167.
- Brunger, A. T. *X-PLOR—a system for X-ray crystallography and NMR*; Yale University Press: New Haven, 1987.
- Zhang, H.; Nimmer, P.; Rosenberg, S. H.; Ng, S. C.; Joseph, M. *Anal. Biochem.* **2002**, 307, 70.
- Oltersdorf, T.; Elmore, S. W.; Shoemaker, A. R.; Armstrong, R. C.; Augeri, D. J.; Belli, B. A.; Brunko, M.; Deckwerth, T. L.; Dinges, J.; Hajduk, P. J.; Joseph, M. K.; Kitada, S.; Korsmeyer, S. J.; Kunzer, A. R.; Letai, A.; Li, C.; Mitten, M. J.; Nettesheim, D. G.; Ng, S.; Nimmer, P. M.; O'Connor, J. M.; Oleksijew, A.; Petros, A. M.; Reed, J. C.; Shen, W.; Tahir, S. K.; Thompson, C. B.; Tomaselli, K. J.; Wang, B.; Wendt, M. D.; Zhang, H.; Fesik, S. W.; Rosenberg, S. H. *Nature* **2005**, 435, 677.
- Porter, J.; Payne, A.; de Candole, B.; Ford, D.; Hutchinson, B.; Trevitt, G.; Turner, J.; Edwards, C.; Watkins, C.; Whitcombe, I.; Davis, J. *Bioorg. Med. Chem. Lett.* **2009**, 19, 230.